Cell Stem Cell
Article

Neurofibromatosis-1 Regulates Neuronal and Glial Cell Differentiation from Neuroglial Progenitors In Vivo by Both cAMP- and Ras-Dependent Mechanisms

Balazs Hegedus,[1] Biplab Dasgupta,[1,3] Jung Eun Shin,[1] Ryan J. Emnett,[1] Elizabeth K. Hart-Mahon,[1] Lynda Elghazi,[2] Ernesto Bernal-Mizrachi,[2] and David H. Gutmann[1,*]
[1]Department of Neurology
[2]Department of Internal Medicine
Washington University School of Medicine, St. Louis, MO 63110, USA
[3]Present address: Department of Pathology, Washington University School of Medicine, St. Louis, MO 63110, USA.
*Correspondence: gutmannd@wustl.edu
DOI 10.1016/j.stem.2007.07.008

SUMMARY

Individuals with neurofibromatosis type 1 (NF1) develop abnormalities of both neuronal and glial cell lineages, suggesting that the *NF1* protein neurofibromin is an essential regulator of neuroglial progenitor function. In this regard, *Nf1*-deficient embryonic telencephalic neurospheres exhibit increased self-renewal and prolonged survival as explants in vivo. Using a newly developed brain lipid binding protein (BLBP)-Cre mouse strain to study the role of neurofibromin in neural progenitor cell function in the intact animal, we now show that neuroglial progenitor *Nf1* inactivation results in increased glial lineage proliferation and abnormal neuronal differentiation in vivo. Whereas the glial cell lineage abnormalities are recapitulated by activated Ras or Akt expression in vivo, the neuronal abnormalities were Ras- and Akt independent and reflected impaired cAMP generation in *Nf1*-deficient cells in vivo and in vitro. Together, these findings demonstrate that neurofibromin is required for normal glial and neuronal development involving separable Ras-dependent and cAMP-dependent mechanisms.

INTRODUCTION

Neurofibromatosis type 1 (NF1) is a common autosomal dominant disorder in which affected individuals develop abnormalities that involve both astrocytes and neurons. In this regard, 20% of children and adults with NF1 develop low-grade astrocytic tumors (gliomas) involving the optic pathway (Listernick et al., 1999). In addition, 40%–60% of children with NF1 exhibit specific learning disabilities with associated low IQ scores (Hyman et al., 2005). Advanced neuroimaging and limited pathologic examination of the brains of affected children have failed to discern a structural basis for these cognitive abnormalities.

The fact that both the astroglial and neuronal lineages are affected in NF1 suggests that the *NF1* gene product neurofibromin may be important for neural stem cell (NSC) or neuroglial progenitor cell function. Support for this notion derives from previous experiments in our laboratory demonstrating that *Nf1*-deficient embryonic telencephalic NSCs exhibited dramatic increases in self-renewal and proliferation (Dasgupta and Gutmann, 2005). Similarly, others have found increased numbers of progenitor cells in the spinal cords from $Nf1^{-/-}$ embryos (Bennett et al., 2003). In addition, $Nf1^{-/-}$ embryos often display a variety of neural tube defects such as exencephaly or thinning of the dorsal telencephalic wall (Lakkis et al., 1999). Using the human GFAP promoter to conditionally inactivate the *Nf1* gene, neurofibromin loss starting between embryonic day (E) 10.5 and E12.5 results in abnormal neurological behaviors and hyperproliferation of glial progenitors (Zhu et al., 2005), whereas neurofibromin loss starting at E14.5 results only in increased astrocyte proliferation (Bajenaru et al., 2002). In contrast, *Nf1* inactivation in a differentiated neuronal population using Synapsin 1 conditional *Nf1* inactivation results in reduced neocortical thickness, less apparent forebrain cortical lamination, and increased cell density (Zhu et al., 2001).

The *NF1* gene encodes a large cytoplasmic protein, neurofibromin, which primarily functions as a negative regulator of the Ras proto-oncogene (DeClue et al., 1992). Loss or reduced neurofibromin expression leads to increased Ras activity as a result of impaired neurofibromin GTPase activating protein (GAP) function. Hyperactivation of the Ras signaling pathway has also been associated with increased mammalian target of rapamycin (mTOR) activity in astrocytes and Schwann cells (Dasgupta et al., 2005; Johannessen et al., 2005). In addition to its ability to inhibit Ras and mTOR activity, neurofibromin is required for intracellular cyclic AMP (cAMP) generation in both neurons and astrocytes (Dasgupta et al., 2003; Tong et al., 2002). In mammalian cells, it is not clear what NF1 disease phenotypes relate to deregulated cAMP generation, prompting recent speculation based

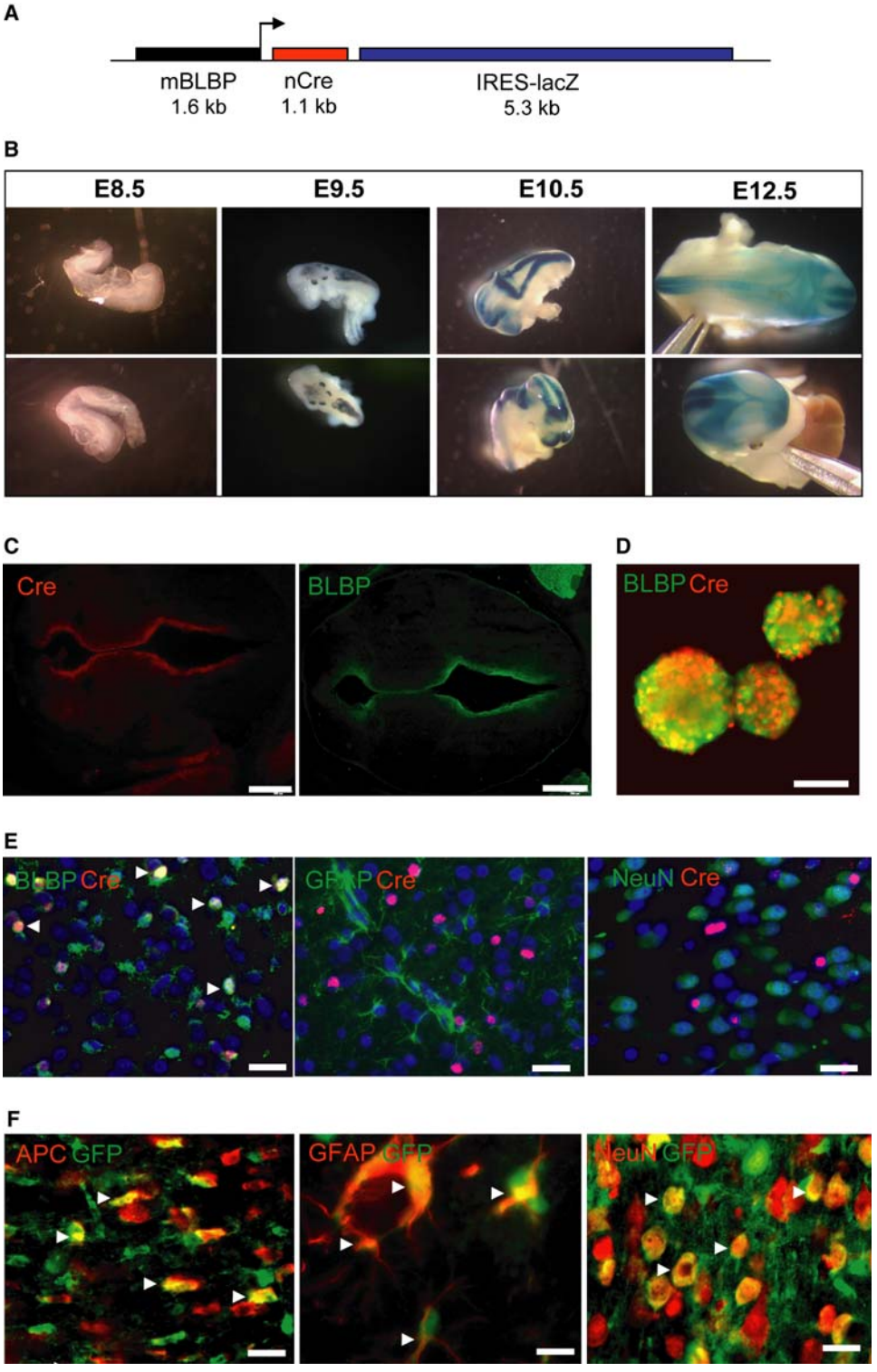

Figure 1. Characterization of BLBP-Cre Transgenic Mice

(A) Schematic of the BLBP-Cre targeting construct.

(B) lacZ expression appears by E9.5 in the spinal cord and hindbrain. From E10.5, lacZ expression is located in the midbrain and rostral forebrain. By E12.5, lacZ expression further extends throughout telencephalon.

(C) Cre expression is restricted to BLBP+ ventricular zone cells in the developing nervous system at E10.5.

(D) E14.5 BLBP+ embryonic neural stem cells exhibit Cre expression in vitro.

on studies in *Nf1*$^{-/-}$ *Drosophila* that neurofibromin does not have separable Ras and cAMP functions (Walker et al., 2006).

To better define the role of neurofibromin in the developing brain and to determine whether neurofibromin has distinct Ras and cAMP functions in the central nervous system (CNS), we chose to inactivate the *Nf1* gene in embryonic neuroglial progenitors. We chose to target brain lipid binding protein (BLBP or Fabp7)-expressing cells in the nervous system based on numerous lines of evidence that suggest that BLBP is expressed in cells with the capacity for self-renewal and multilineage differentiation. BLBP is robustly expressed in the major adult neurogenic regions, including in the subventricular zone (Sundholm-Peters et al., 2004), spinal cord (Taylor et al., 2005), and germinal layer of the dentate gyrus (Kurtz et al., 1994). Moreover, BLBP expression is found in embryonic and adult NSC neurosphere cultures capable of self-renewal and multilineage differentiation (Dromard et al., 2006). Based on these observations, we generated transgenic mice that express Cre recombinase under the control of a fragment of the mouse BLBP promoter (Arnold et al., 1994).

In this study, we show that loss of neurofibromin in BLBP+ cells in vivo results in increased proliferation of neuroglial progenitor cells during embryogenesis and leads to an expansion of glial progenitors as well as mature astrocytes in a Ras- and Akt-dependent fashion. In addition, neurofibromin is necessary for normal neuronal differentiation and forebrain cortical development, which reflects the ability of neurofibromin to positively regulate intracellular cAMP levels. This unique *Nf1* mouse model provides a valuable tool to study the neuronal and glial abnormalities associated with the human disease and to define how defects in Ras and cAMP signaling regulate progenitor cell differentiation in vivo.

RESULTS

Development and Characterization of BLBP-Cre Transgenic Mice

In order to inactivate the *Nf1* gene in embryonic neuroglial progenitor cells, mice were generated that express nuclear-targeted Cre recombinase under the control of a 1.6 kb fragment of the mouse BLBP promoter (Arnold et al., 1994). This expression construct also contains an IRES-lacZ sequence to allow for detection of BLBP promoter activity in the developing embryo by X-gal staining (Figure 1A). Three independent founders were identified by PCR and used to establish BLBP-Cre transgenic lines. Analysis of lacZ activity in the resulting embryos and adult mice showed that lines #2 and #3 displayed identical spatiotemporal expression patterns. These two lines were used interchangeably in the present study.

We employed several methods to characterize Cre expression and activity in the nervous system of BLBP-Cre mice. First, β-galactosidase expression was detected along the ventricular region of the spinal cord and in the hindbrain by E9.5. At E10.5, lacZ activity appeared in the dorsal portion of the rostral neuroepithelium and in the midbrain. By E12.5, the β-galactosidase activity extended into the ventricular/subventricular regions of the brain (Figure 1B). No lacZ activity was found in any other organ system. In young adult mice, lacZ activity was detected in the ependymal cell layer of the ventricle with distinct cellular labeling in the subventricular zones as well as in the subgranular zone of the dentate gyrus (data not shown). Second, to demonstrate that Cre recombinase expression was detected in embryonic cells with endogenous BLBP expression, we labeled BLBP- and Cre-expressing cell populations in transverse sections of the neural tube by immunofluorescence. Transgenic Cre expression was coincident with endogenous BLBP expression in the ventricular region (Figure 1C). Third, to demonstrate that Cre recombinase was expressed in neuroglial progenitor cells, we generated neurospheres from BLBP-Cre embryos (E12.5 and E14.5) and neonatal mice. As in the intact embryonic ventricular zone, both endogenous BLBP and transgenic Cre recombinase expression were detected in embryonic and postnatal neurospheres (Figure 1D and Figures S1A and S1B in the Supplemental Data available with this article online) that were capable of self-renewal (data not shown) and multilineage differentiation (Figure S1C). Fourth, we analyzed Cre recombinase expression in BLBP-Cre mice by immunofluorescence at postnatal day 18 (PN18). No GFAP+ astrocytes or NeuN+ neurons contained Cre+ nuclei. However, > 90% of Cre+ cells expressed BLBP (Figure 1E). Finally, to assess Cre recombinase activity, we crossed BLBP-Cre mice with the R26R-EYFP reporter strain (Srinivas et al., 2001). At PN18, the majority of APC+ oligodendrocytes in the fimbria, GFAP+ astrocytes in the CA1 region of the hippocampus, and NeuN+ neurons in the cortex were colabeled by an antibody against EYFP (Figure 1F). No EYFP expression was detected outside of the nervous system. Collectively, these results demonstrate that Cre recombinase is expressed in BLBP+ cells in the embryonic (and adult) ventricular zone capable of self-renewal and multilineage differentiation.

Generation of *Nf1* Conditional Knockout Mice

In order to evaluate the role of neurofibromin in the developing CNS, BLBP-Cre mice were intercrossed with *Nf1*$^{flox/flox}$ mice (Zhu et al., 2001). BLBP-Cre;

(E) At PN18, only BLBP+ progenitor cells express Cre recombinase (arrowheads) in the subventricular zone. No Cre recombinase expression was present in GFAP+ cells (astroglial) in the hippocampus or in cortical NeuN+ cells (neurons).
(F) EYFP expression is present in all major cell types of the brain, including APC+ oligodendrocytes from the fimbria, GFAP+ astrocytes in the hippocampus, and NeuN+ neurons of the cortex of R26R-EYFP × BLBP-Cre mice (indicated by arrowheads).
Scale bars: (C), 250 μm; (D), 100 μm; (E), 50 μm; and (F), 25 μm.

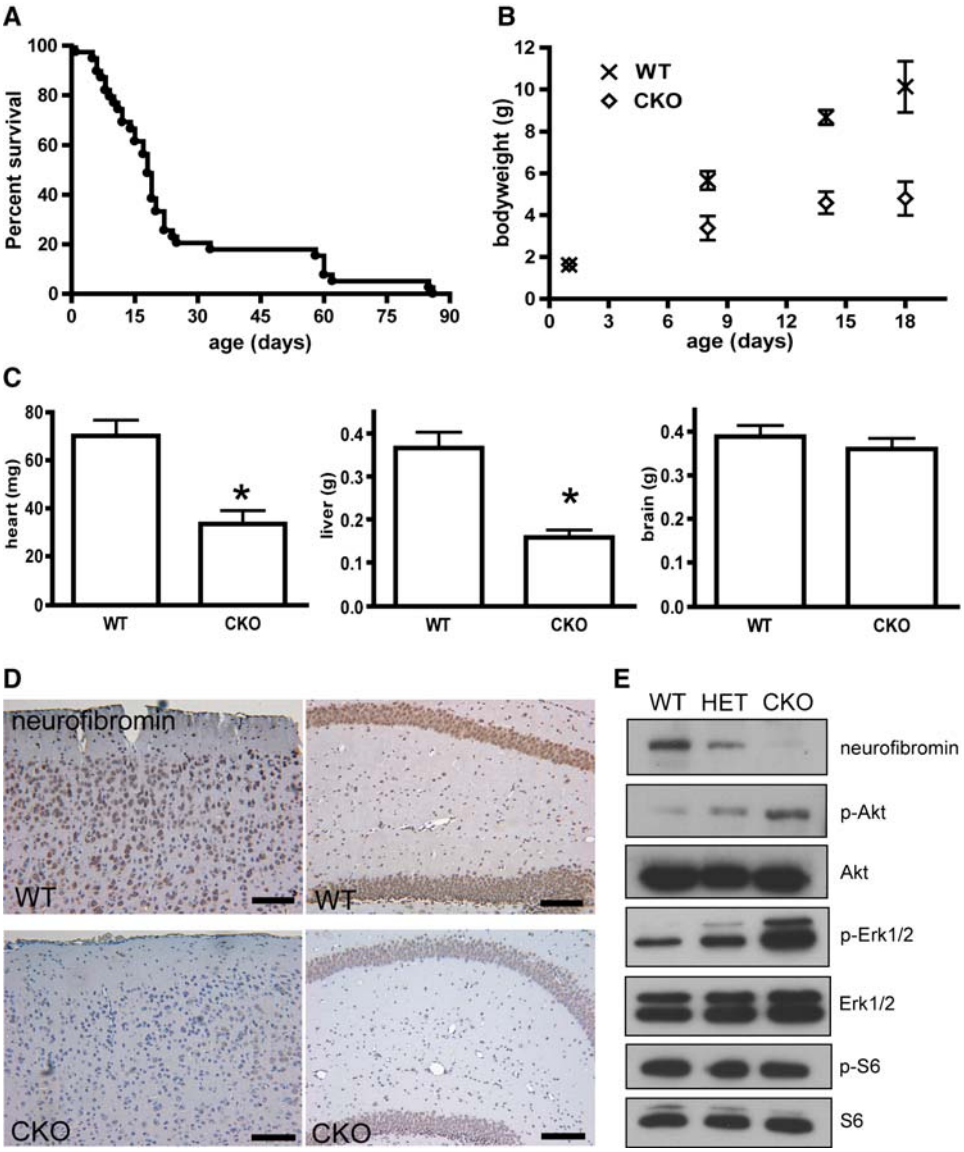

Figure 2. Neurofibromin Loss in the Brain Results in Dwarfism and Premature Death

(A) CKO mice have a median survival of 18 days.

(B) Growth retardation appears within 7 days after birth. Values represent mean and standard error of measurement (SEM).

(C) Significant weight reduction of the heart and liver was observed, while the slight reduction in brain weight was not statistically significant. Error bars denote SEM.

(D) Neurofibromin expression was decreased in the cortex and hippocampus of CKO mice by immunohistochemistry and western blot. Scale bar, 100 μm.

(E) Increased activation of Akt and Erk1/2, but not S6, was detected. Asterisks denote a statistically significant difference ($p < 0.05$).

Nf1$^{flox/wt}$ × *Nf1*$^{flox/flox}$ crossings resulted in progeny with the expected Mendelian ratios in utero and at birth. BLBP-Cre; *Nf1*$^{flox/flox}$ (CKO), BLBP-Cre; *Nf1*$^{flox/wt}$ (HET), as well as BLBP-Cre, *Nf1*$^{flox/flox}$ and *Nf1*$^{flox/wt}$ (WT) mice were indistinguishable by appearance at PN1. However, CKO mice developed progressive growth retardation from PN3 and the majority of the pups failed to survive to weaning. CKO mice displayed limited range of movement of the rear legs and an extreme sensitivity to handling. Brain electric activity was monitored by implanted electrodes during a 24 hr observation period and no seizures were observed (M. Wong, personal communication). Median survival for CKO mice was 18 days, and no mice survived longer than 3 months (Figure 2A). At PN18, the weight of the surviving CKO mice was less than 50% that of their control littermates (Figure 2B). All the major organ systems displayed growth retardation, except for the CNS. Eighteen days after birth, we found a significant decrease in the weight of the heart and liver (Figure 2C), as well as of the spleen, kidney, and testis (data not shown). However, complete autopsy and histological analysis of two representative PN18 CKO mice

did not identify any structural or histological abnormalities in these organs (data not shown). There was a 7% reduction in the weight of CKO brains at PN18, which was not statistically significant ($p = 0.08$). The exact cause of death is not known.

Loss of neurofibromin expression in CKO brains was demonstrated by immunohistochemistry (Figure 2D) at PN18 as well as by western blotting of forebrain lysates from newborn mice (Figure 2E). Because neurofibromin is a major regulator of Ras, the activation of Ras downstream targets was measured. In agreement with previous studies, we found gene dose dependent increased activation of Akt and ERK1/2 with activation-specific antibodies (Figure 2E). In contrast, we observed no hyperactivation of the mTOR downstream target S6. Immunohistochemistry with phospho-specific S6 antibodies showed no differences between CKO and wild-type (WT) mice (Figure S2A), whereas there were increased numbers of phospho-Erk1/2-labeled cortical pyramidal neurons in CKO compared to WT brains (Figure S2B).

Increased Glial Cell Populations in CKO Mice

To evaluate the effect of neurofibromin loss in embryonic neuroglial progenitor cells on multilineage differentiation, immunohistochemical labeling for neuronal, astroglial, and oligodendroglial markers was performed at PN18. All major anatomical regions in the forebrain appeared normal as demonstrated by the number of NeuN+ neurons, the presence of MAP2+ neuronal processes, as well as the extent of myelin basic protein (MBP) expression by oligodendrocytes (Figure 3A). However, we observed increased numbers of GFAP+ astrocytes and NG2+ glial cells as well as APC+ oligodendroglial cells in the CKO brains (Figure 3B). We quantified the number of GFAP+ cells in high-power fields of the CA1 region of the hippocampus and found a significant *Nf1* gene dose-dependent increase in CKO and HET brains compared to WT brains. Similarly, the number of APC+ cells in the fimbria as well as the number of NG2+ cells in the somatosensory cortex was significantly higher in the CKO mice. The number of NG2+ cells was higher in HET mice compared to wild-type animals; however, this increase was not statistically significant ($p = 0.1$). There was no difference in the number of NeuN+ cells in the primary somatosensory cortex or in the granular cell layer of the hippocampus between CKO and WT mice (data not shown). These findings demonstrate that loss of neurofibromin in the neuroglial progenitor cells in vivo leads to an expansion of glial, but not neuronal, cell populations.

We next sought to determine whether BLBP-mediated *Nf1* loss results in increased proliferation of neuroglial progenitor cell populations in vivo. For these experiments, timed-pregnant mice were injected with bromodeoxyuridine (BrdU) 1 hr prior to euthanasia at E13.5 and E17.5. Frozen sections of embryonic brains were labeled for BrdU and markers of neuroglial and neuronal progenitors (Figure 4A). Increased BrdU incorporation was observed in the ventricular zone of CKO embryos at E13.5 and to a lesser extent at E17.5. Almost all BrdU incorporating cell in the embryonic ventricular zone expressed Sox2, a marker of proliferating neuroglial progenitor cells (Figure S3A). We also found increased numbers of Sox2+ and vimentin+ (neural stem cell/progenitor marker) cells around the lateral ventricles of E13.5 CKO embryos. However, there was no difference in the thickness of the cortical plate between CKO and WT mice using the neuronal precursor markers Tuj1 and doublecortin (data not shown). Postnatally, there was no difference in the number of BrdU+ or Sox2+ cells in the dentate gyrus and the subventricular zone (SVZ) of the lateral ventricles where adult neural stem cells reside (Figure 4A and Figure S3B).

Previous studies have shown that neurofibromin regulates proliferation in the brain (Zhu et al., 2005). To determine whether *Nf1* inactivation in neuroglial progenitors resulted in increased cell proliferation in the postnatal period, we analyzed proliferation in 1-week-old mice injected with BrdU. We found increased numbers of proliferating cells in the CA2/3 region of the hippocampus in both HET and CKO mice compared to WT animals. Using antibodies against BLBP and Olig2, a major transcription factor regulating glial differentiation (Ligon et al., 2006), we observed increased numbers of Olig2+ glial and BLBP+ neuroglial progenitors throughout the brains of CKO mice (Figures 4B and 4C). However, after normalization to the total Olig2+ (or BLBP+) progenitor cell number, there was no increase in the percentage of proliferating Olig2+ (or BLBP+) cells, indicating that the increased proliferation reflects an increase in the total number of progenitor cells resulting from *Nf1* loss. Consistent with previous studies on $Nf1^{-/-}$ astrocytes (Bajenaru et al., 2002), astroglial cultures established from PN1 CKO mice exhibited increased proliferation by BrdU and $[^3H]$-thymidine incorporation (Figure S3C). No difference in the number of apoptotic cells labeled by activated caspase-3 immunostaining or TUNEL staining was seen (data not shown). Collectively, these data demonstrate that neurofibromin expression in neuroglial progenitors is required for proper glial cell differentiation and proliferation.

Loss of Neurofibromin Results in Abnormal Neurite Development

Because previous studies using Synapsin 1 conditional *Nf1* knockout mice implicated neurofibromin in cortical development, we analyzed the brains of PN18 CKO mice for defects in neuronal maturation. Using Golgi staining, we found grossly normal organization of neuronal processes in the brains of CKO mice (Figure 5A). However, the apical dendrites of the layer II/III pyramidal neurons in the somatosensory cortex were shorter in CKO compared to WT or HET animals (Figure 5B). Interestingly, when embryonic (E10.5) $Nf1^{-/-}$ neurospheres undergo neuronal differentiation in vitro, the resulting neurons also exhibited shortened neurite processes (Figure 5C). In contrast to the results obtained in vivo, there was a gene dose-dependent decrease of neurite length in $Nf1^{+/-}$ and $Nf1^{-/-}$ differentiated NSC cultures in vitro (Figure 5D).

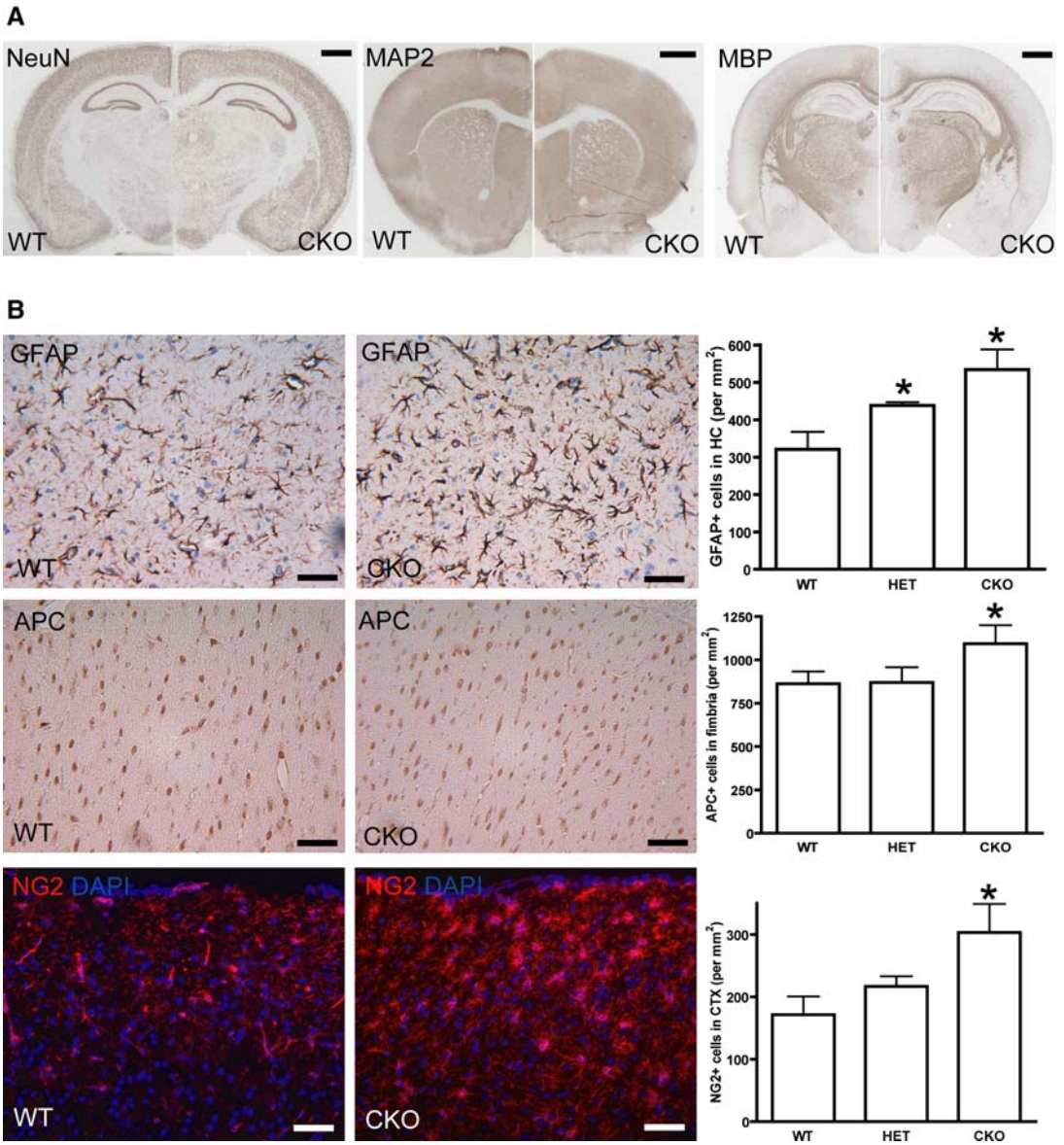

Figure 3. CKO Brains Display Proper Anatomical Organization but Exhibit Increased Numbers of Glial Cells

(A) Coronal brain sections reveal a normal abundance of NeuN+ neurons, MAP2+ neuronal processes, and myelin basic protein (MBP).

(B) In CKO mice, increased density of GFAP+ cells was found in the CA1 region of hippocampus. HET exhibited an intermediate increase in cell density. The number of oligodendrocytes was also significantly higher in the high-power fields of coronal sections of fimbria of CKO brain compared to WT or HET mice. The density of cortical NG2+ glial cells was increased in the CKO mice. Values represent mean ± SEM.

Scale bars: (A), 1 mm; (B), 100 μm. Asterisks denote a statistically significant difference ($p < 0.05$).

Based on these observations, we hypothesized that there might be a delay in cortical neuron maturation. To better characterize this defect, we examined markers associated with neuritogenesis and dendritic development at PN1. We found decreased numbers of thick fibers labeled by antibodies against MAP2, a microtubule-associated protein found in dendrites (Figure 5E). There was also reduced expression of GAP43, a developmentally regulated growth cone-associated protein in the developing cortex of CKO mice by immunofluorescence labeling (Figure 5E) as well as by western blot (Figure 5F). We also observed decreased expression of a phosphorylated form of the neurofilament heavy chain that is normally increased during neuronal differentiation (Figure 5F). In contrast, we found no differences in the expression of the major proteins associated with presynaptic structures, including synapsin 1 or synaptophysin (Figure 5F). Taken together, these findings suggest that neurofibromin is necessary for the normal development and differentiation of neocortical neurons.

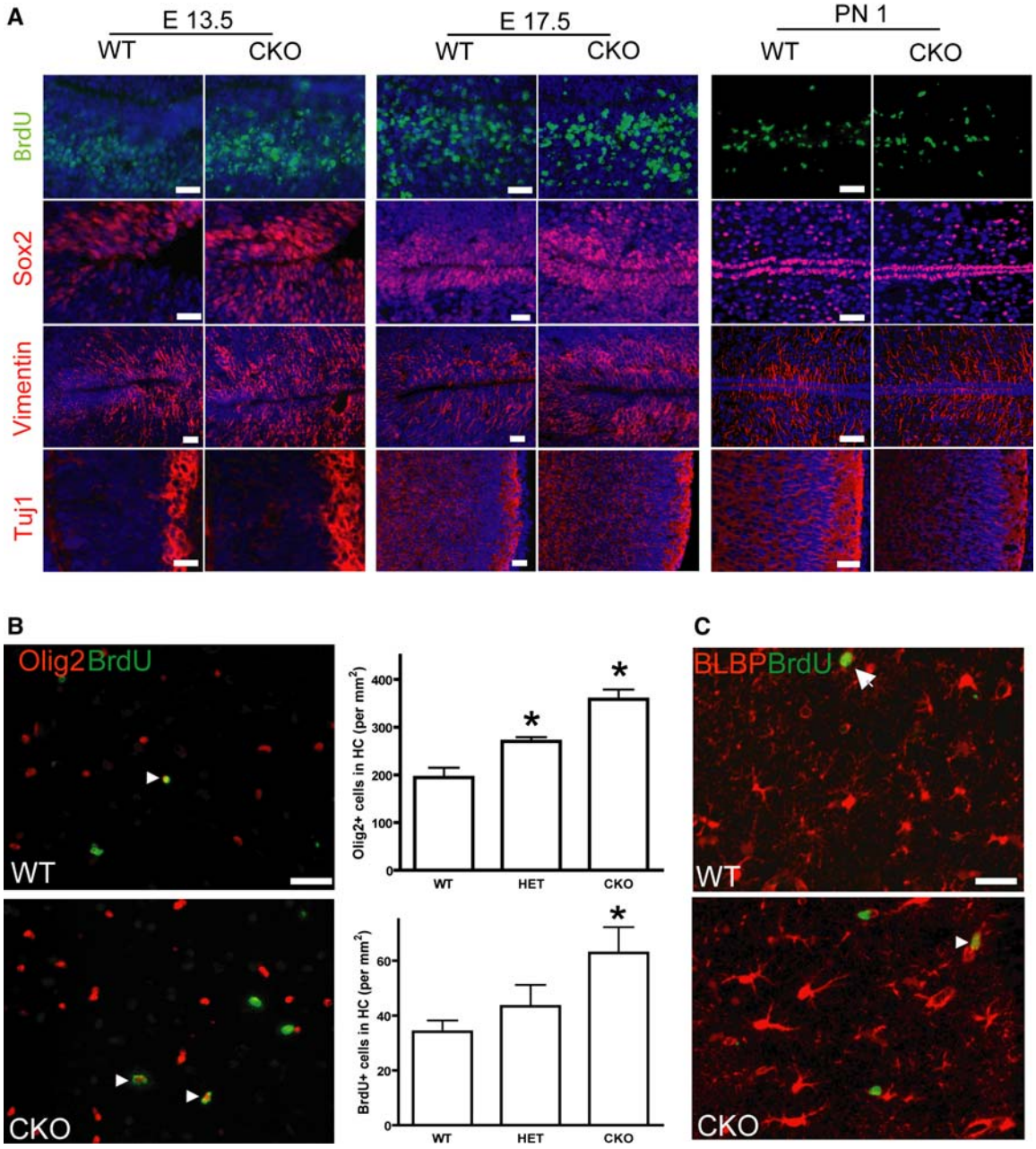

Figure 4. Embryonic Loss of Neurofibromin Results in Increased Neuroglial Progenitor Cell Numbers

(A) Increased BrdU incorporation as well as increased numbers of Sox2+ and vimentin+ cells were observed in CKO brains at E13.5. There was no difference in the pattern of Tuj1 labeling in the cortical plate.

(B) At PN8, increased numbers of Olig2+ glial progenitor cells were found throughout the brain (HC, hippocampus). There was an increase in proliferating cells in the same region; however, no differences were found in the ratio of proliferating (BrdU+), Olig2+ cells in CKO and HET brains compared to WT mice. Values represent mean ± SEM.

(C) A number of the proliferating cells expressed the progenitor marker BLBP.

Scale bars: (A), 100 μm; (B), 50 μm. Asterisks denote a statistically significant difference ($p < 0.05$). Arrowheads show double-labeled cells.

Abnormal Glial, but Not Neuronal, Phenotypes in CKO Mice Reflect Ras Activation

The major function of neurofibromin is to negatively regulate Ras activity. To recapitulate Ras activation resulting from neurofibromin loss in neuroglial progenitor cells, we employed LSL-KRas^{G12D} mice (Johnson et al., 2001). For these studies, BLBP-Cre and Lox-stop-lox (LSL)-KRas^{G12D} mice were intercrossed to generate BLBP-Cre; LSL-KRas^{G12D} (Kras*) mice. Kras* were viable and lacked the severe growth retardation, abnormal

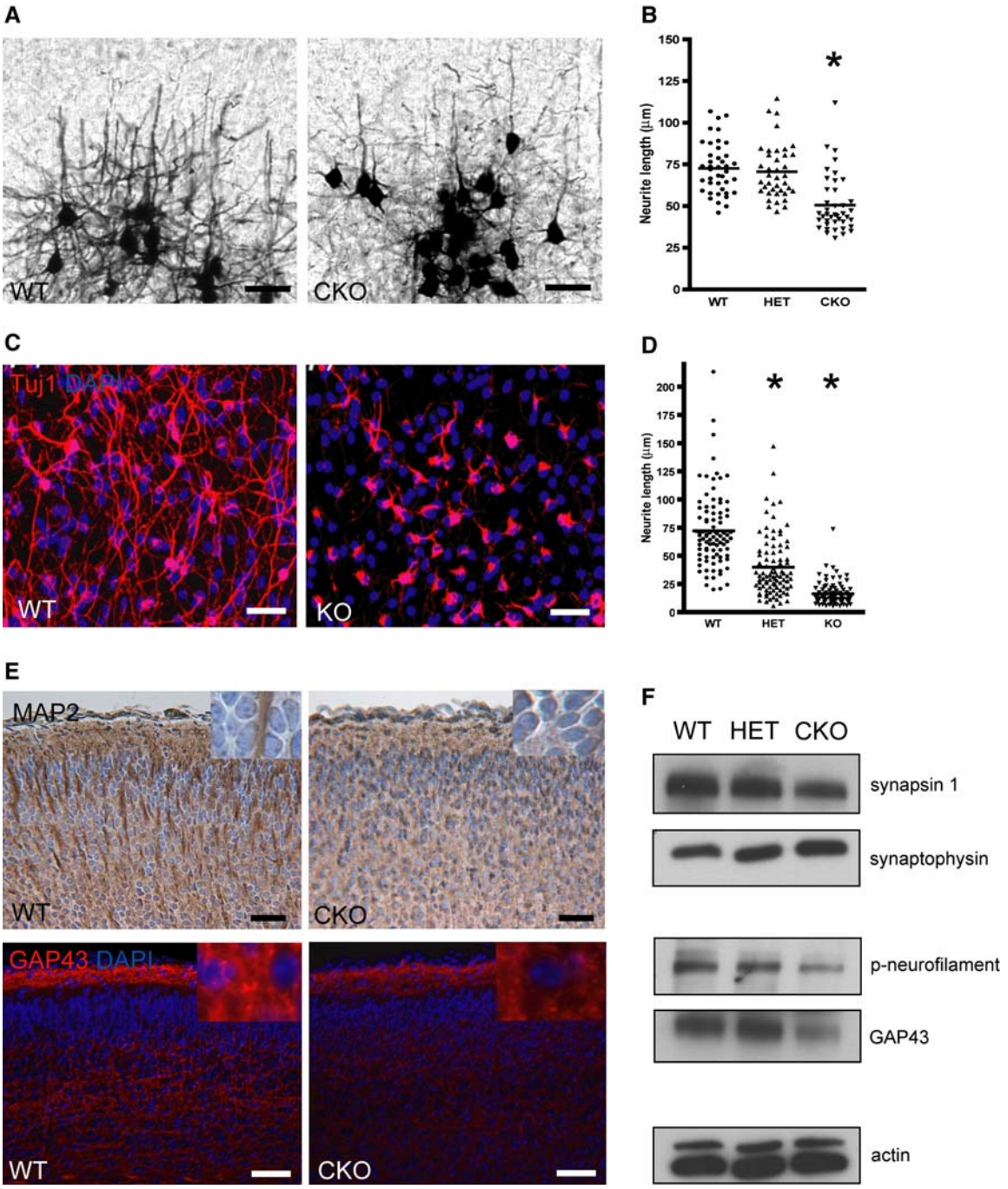

Figure 5. Loss of Neurofibromin in Neuroglial Progenitor Cells Impairs Neuronal Differentiation

(A and B) Golgi staining of brains at PN18 demonstrated that the apical dendrites of pyramidal neurons were significantly shorter in CKO mice compared to WT or HET animals.

(C and D) *Nf1*$^{-/-}$ and *Nf1*$^{+/-}$ embryonic NSCs stimulated to undergo differentiation in vitro generated neurons with significantly shorter Tuj1+ neurites.

(E) Decreased number of thick MAP2+ processes and less intense GAP43 staining was apparent in the cortex of PN1 CKO pups.

(F) Western blot analysis demonstrates reduced expression of phospho-neurofilament and GAP43 in PN1 brain lysates. No changes in synapsin 1 or synaptophysin were seen.

Scale bars: (A), 25 μm; (C), 30 μm; and (E), 100 μm. Asterisks denote a statistically significant difference ($p < 0.05$).

behaviors, or reduced survival observed in the CKO mice (Figure 6A). Histological analysis of Kras* brains revealed an expansion of glial cell populations similar to that observed in CKO mice, with more GFAP+ and NG2+ glial cells and Olig2+ progenitor cells compared to WT mice (Figure 6B and Figure S4A). Similar to CKO mice, there

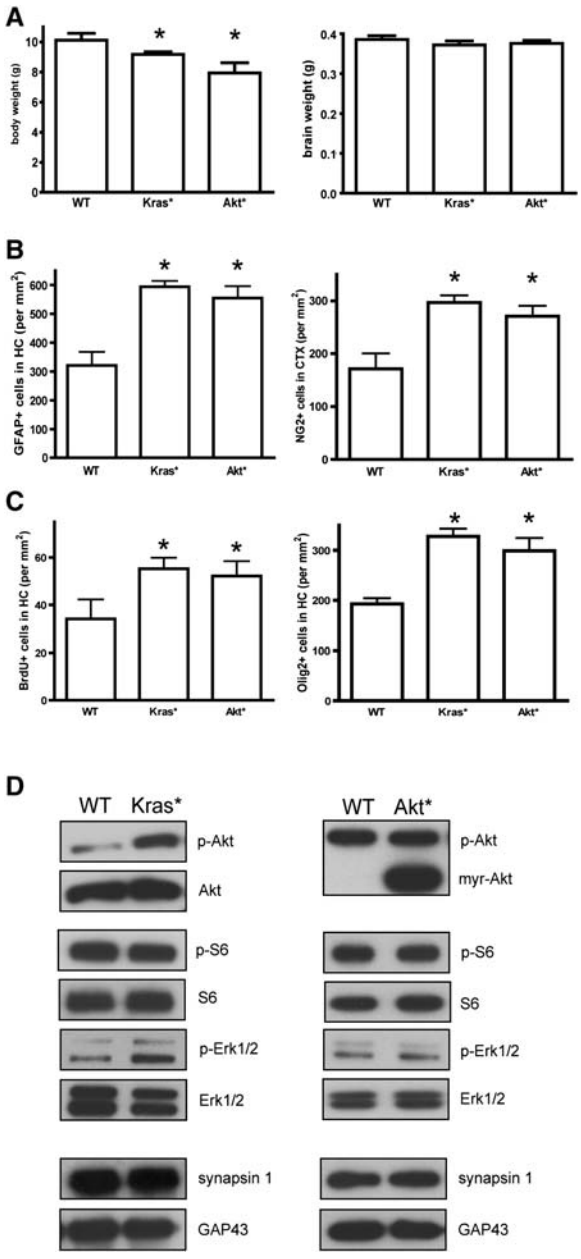

Figure 6. Increased Glial Progenitor Numbers, but Not Neocortical Neuronal Development, Is Kras- and Akt Dependent

(A) BLBP-Cre; LSL-KRas^{G12D} (Kras*) and BLBP-Cre; LSL-myr-Akt (Akt*) mice develop normally, and their brain weights are similar to WT mice. There is a slight decrease in Kras* and Akt* body weights at PN18 ($p = 0.01$).

(B) The number of NG2+ and GFAP+ cells is significantly higher in the cortex and hippocampus of Kras* and Akt* mice, respectively.

(C) There is an increase in the number of BrdU incorporating as well as Olig2+ cells in the hippocampus.

(D) Kras activation results in Erk1/2 and Akt activation but did not change the expression of proteins involved in neuronal development (synapsin I and GAP43). In the Akt* mice, there was abundant expression of the constitutively active form of Akt but there was no increase in the activation status of Erk1/2 and S6.

Asterisks denote a statistically significant difference ($p < 0.05$). Values represent mean ± SEM.

were also more BrdU+ cells in the CA2/3 region of Kras* mice than in littermate controls (Figure 6C). However, Golgi staining of Kras* brains did not demonstrate any changes in pyramidal neuron apical dendrite lengths (Figure S4B). Moreover, we did not observe any changes in the expression of markers associated with neuritic development (Figure 6D) or reduced forebrain cortical thickness (Figure 7C) in Kras* mice.

One major downstream target of Ras is Akt. In order to determine whether the brain abnormalities observed in the CKO or Kras* mice could be recapitulated by constitutive Akt activation, we generated BLBP-Cre; LSL-myr-Akt (Akt*) mice. Similar to Kras* mice, Akt* mice were viable and did not exhibit severe growth retardation, abnormal behaviors, or reduced survival. Akt* mice had more GFAP+ and NG2+ glial cells and Olig2+ progenitor cells compared to WT mice (Figure 6B) as well as increased numbers of BrdU+ cells in the CA2/3 region (Figure 6C). Moreover, Akt* mice had normal forebrain cortical thickness (Figure 7C). Interestingly, similar to CKO mice, Kras* and Akt* mice did not exhibit increased S6 activation in the brain (Figure 6D).

Collectively, these results demonstrate that constitutive activation of Kras or Akt recapitulates the glial cell defects associated with neurofibromin loss in neuroglial progenitors but does not account for the abnormalities in neuronal differentiation observed in CKO mice.

Neurofibromin Regulates Cortical Development in a cAMP-Dependent Manner

Previous studies have shown that, in addition to its ability to negatively regulate Ras, neurofibromin positively controls cAMP generation in astrocytes and neurons (Dasgupta et al., 2003; Tong et al., 2002). The inability of Kras or Akt activation to recapitulate the neuronal defects observed in CKO mice raised the intriguing possibility that neurofibromin cAMP regulation may underlie the abnormalities in neuronal differentiation. In support of cAMP-dependent effects, we found a significant decrease in the total levels of intracellular cAMP in CKO brains (Figure 7A). This reduction in cAMP levels was reflected in reduced CREB activation in CKO, but not HET or WT, mouse brains (Figure 7B and Figure S5A). No decrease in CREB activity was seen in Kras* or Akt* mouse brains.

To investigate whether neurofibromin regulates forebrain cortical development and neurite length in a cAMP-dependent manner, we employed a specific inhibitor of phosphodiesterase-4 (PDE4) to increase cAMP levels in vivo. Rolipram acts to inhibit PDE4-mediated degradation of cAMP and has been used to elevate cAMP in the CNS (Barad et al., 1998; Giorgi et al., 2004). Previous studies have shown that the thickness of the secondary somatosensory cortex is markedly reduced in mice lacking neurofibromin in neurons (Zhu et al., 2001). As reported for the *Nf1*^{Synl}CKO mice, the distance between the corpus callosum and the brain surface in the secondary somatosensory cortex was significantly reduced in CKO mice. Rolipram was administered daily by intraperitoneal injection from E11.5 to PN18 to the mother

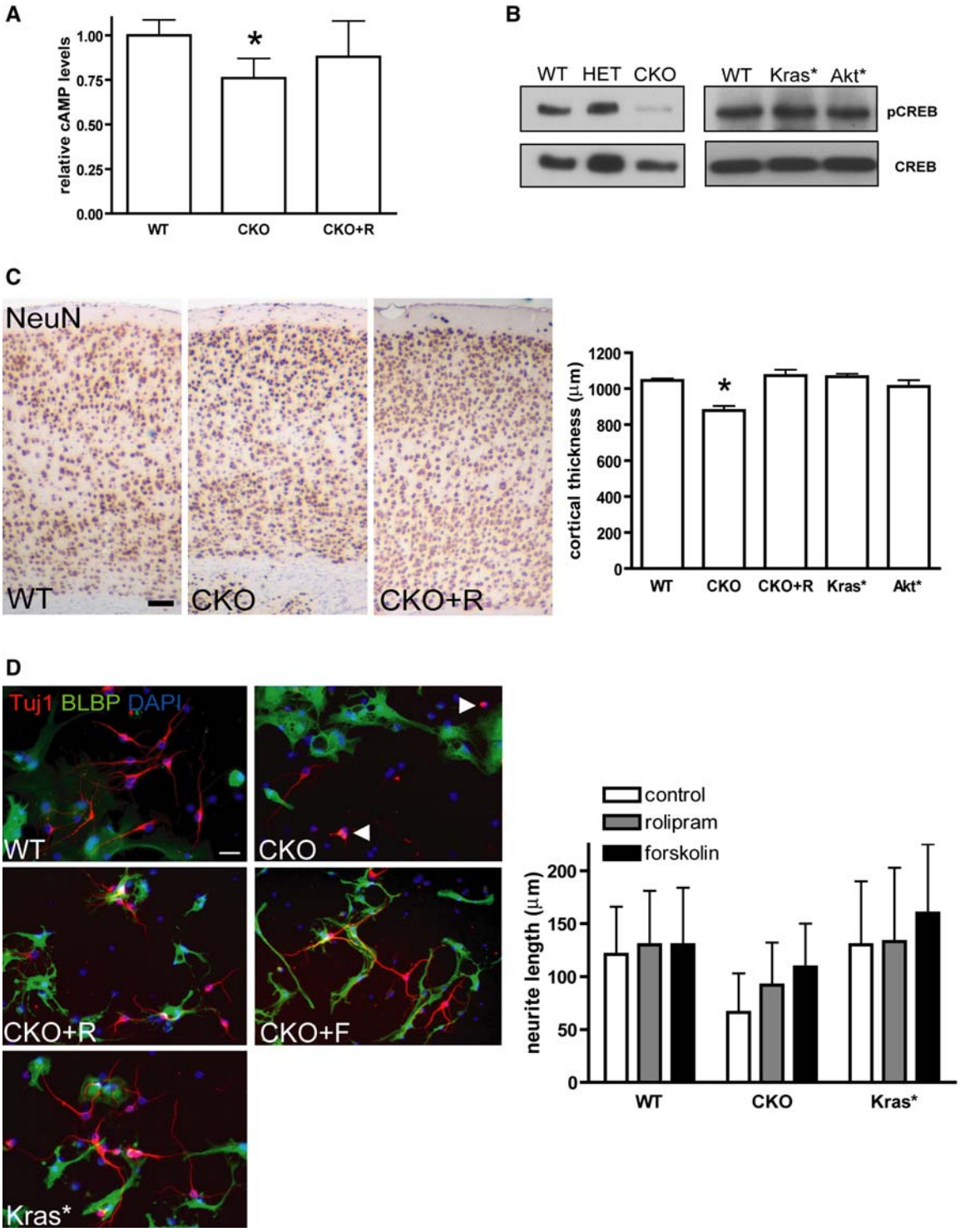

Figure 7. Neurofibromin Regulation of Cortical Development Is cAMP Dependent

(A) Cyclic AMP levels were lower in CKO compared to WT brains ($p = 0.02$). Rolipram administration increased cAMP levels in CKO brains. Error bars denote SEM.

(B) Activation of CREB was decreased in CKO, but not in HET, Kras*, or Akt* mice compared to WT controls.

(C) The thickness of the somatosensory cortex of CKO mice was reduced compared to WT mice. Rolipram treatment restored the cortical thickness in CKO mice (CKO+R) to that seen in WT mice. Values represent mean ± SEM.

(D) Impaired neurite extension in differentiating CKO neural progenitors ($p < 0.0001$, arrowheads show cells with short neurites) was partially rescued by rolipram treatment ($p = 0.04$ compared to untreated CKO cells; $p = 0.014$ compared to WT cells), whereas forskolin nearly completely rescued the

as well as beginning at PN7 to the pups directly, and the resulting mice were euthanized at PN18. Rolipram-treated, but not untreated, mice exhibited cortical thickness similar to that observed in wild-type mice (Figure 7C). Furthermore, Golgi staining revealed that rolipram treatment partially restored the length of cortical pyramidal neuron apical dendrites in the somatosensory cortex of CKO mice to that seen in wild-type animals (Figure S6C). Importantly, rolipram-treated CKO mice exhibited similar increases in Akt and ERK activation as well as glial cell expansion compared to untreated mice (Figures S5D and S5E).

In order to demonstrate that impaired cAMP generation in CKO mice accounted for the defects in neurite length, we quantified neurite lengths of neurons generated from E14.5 secondary neurospheres in vitro. After 7 days, we observed a significant decrease in maximal neurite length in CKO compared to WT neurons ($p < 0.0001$; Figure 7D). In contrast, neurite lengths in Kras* or Akt* (data not shown) neurosphere-derived neurons were indistinguishable from WT cultures. Next, we treated cultures with either rolipram or forskolin to increase intracellular cAMP levels. We found that rolipram treatment (20 μM) partially restored the CKO neurite growth defect ($p = 0.04$ compared to untreated CKO cells; $p = 0.014$ compared to WT cells), whereas forskolin treatment (20 μM) nearly completely rescued this defect in vitro ($p = 0.003$ compared to untreated CKO cells; $p = 0.28$ compared to WT cells). No effect of rolipram or forskolin was seen on WT cultures. Collectively, these results demonstrate that neurofibromin regulates neuronal development in a cAMP-dependent and Ras-independent manner.

DISCUSSION

This study demonstrates an essential role for the *Nf1* gene in neural progenitor cell function, astroglial growth regulation, and neuronal differentiation. In CKO mice, we found increased numbers of glial progenitors as well as mature astrocytes and oligodendrocytes. These results are consistent with previous studies from our laboratory in which *Nf1* inactivation in glial progenitors at E14.5 leads to increased astrocyte proliferation in vitro and in vivo (Bajenaru et al., 2002). Similarly, glial progenitor *Nf1* inactivation between E10.5 and E12.5 results in increased numbers of immature GFAP+/nestin+ cells as well as increased numbers of proliferating GFAP+ cells in vivo (Zhu et al., 2005). It is important to note that the increased proliferation observed postnatally is the result of the increased specification of glial progenitors rather than the increased rate of glial progenitor proliferation (e.g., due to shortened cell-cycle length, etc.). This observation suggests that neurofibromin regulates neural stem/progenitor cell differentiation. It is likely that neurofibromin is an important determinant of stem cell/progenitor cell self-renewal and differentiation, such that *Nf1* loss results in an inappropriate persistence of immature progenitors in the brain. In keeping with the cancer stem cell hypothesis (Singh et al., 2004), this delay in glial progenitor maturation could predispose to the development of glial cell tumors. In this regard, preliminary analysis of the limited number of mice that survived to 2–3 months of age indicates that *Nf1* loss in BLBP+ progenitor cells leads to cellular changes in the prechiasmatic optic nerve suggestive of neoplasia.

Neurofibromin is also involved in the regulation of oligodendrocyte precursor cells in the embryonic $Nf1^{-/-}$ spinal cord (Bennett et al., 2003). We previously reported increased oligodendrocyte numbers upon $Nf1^{-/-}$ NSC differentiation in vitro (Dasgupta and Gutmann, 2005). In the current study, we also observed increased numbers of APC+ cells in CKO mice, supporting the observation that *Nf1* loss impairs both astrocyte and oligodendrocyte differentiation. However, we did not observe a statistically significant gene dose effect of *Nf1* loss in NG2+ glial cells, APC+ oligodendrocytes, or Olig2+ glial progenitors. These findings suggest that astrocytes may be most sensitive to changes in *Nf1* gene expression and may underlie the increased frequency of GFAP+ astrocytic tumors in individuals with NF1.

The high incidence of cognitive dysfunction in NF1 patients suggests that neurofibromin is also necessary for normal neuronal development. Importantly, $Nf1^{+/-}$ mice exhibit learning deficits (Silva et al., 1997), whereas complete loss of *Nf1* in certain neuronal cell populations leads to severe behavioral abnormalities (Zhu et al., 2005). The impact of *Nf1* loss on neuronal development was first described in $Nf1^{-/-}$ embryos that displayed hyperplasia of neural crest-derived para- and prevertebral ganglia (Brannan et al., 1994). In vitro, $Nf1^{-/-}$ embryonic peripheral neuronal cell cultures exhibited nerve growth factor (NGF)-independent survival (Klesse and Parada, 1998; Vogel et al., 1995). Using Synapsin I to target *Nf1* inactivation to neurons, neurofibromin loss resulted in increased plasticity following peripheral nerve injury (Romero et al., 2007).

However, in the CNS, neurofibromin loss in these same $Nf1^{SynI}$CKO mice resulted in decreased cortical thickness without any change in the number of cortical neurons (Zhu et al., 2001), similar to $Nf1^{BLBP}$CKO mice. In addition, we found that *Nf1* loss in neural stem/progenitor cells also impairs apical dendrite length in vivo and neurite extension in vitro. Consistent with decreased neurite length, we found reduced expression of proteins involved in neuronal process development, such as phosphorylated neurofilament and GAP43 (Jacobson et al., 1986; Shea et al., 1997). The decrease in GAP43 expression is interesting in light of the established role of this protein in neuronal plasticity (Benowitz and Routtenberg, 1997), suggesting a role in memory

neurite length deficit ($p = 0.003$ compared to untreated CKO cells; $p = 0.28$ compared to WT cells). Neurite lengths in cells cultured from Kras* embryos were indistinguishable from WT cultures. Error bars denote standard deviation.
Scale bars: (C), 100 μm; (D), 20 μm. Asterisks in (A) and (C) denote a statistically significant difference ($p < 0.05$).

and learning, the two major cognitive functions impaired in NF1 patients and $Nf1^{+/-}$ mice.

Neurofibromin is a major regulator of Ras-dependent signaling by virtue of its ability to stimulate the conversion of the GTP-bound active Ras to the GDP-bound inactive form (Basu et al., 1992; DeClue et al., 1992). To define the mechanism underlying neurofibromin regulation of neuroglial progenitor function, we used two approaches. The first approach involved the use of mice with BLBP+ cell expression of an activated Kras or Akt allele. Kras hyperactivation, similar to constitutive activation of Akt, in neuroglial progenitors in vivo recapitulated the glial cell phenotypes observed in CKO mice, but not the neuronal abnormalities. Second, we attempted to rescue the glial cell defects in CKO mice in vivo by using rolipram to block phosphodiesterase-4 (PDE4)-mediated cAMP degradation and increase intracellular cAMP levels. However, we did not observe restoration of glial cell numbers or proliferation after rolipram treatment. These findings suggest that neurofibromin regulates gliogenesis from progenitor cells in a Ras- and Akt-dependent, but cAMP-independent, manner.

Another important downstream target of Ras is mTOR, a major regulator of protein synthesis, previously shown by ourselves and others to be hyperactivated in $Nf1^{-/-}$ astrocytes and Schwann cells (Dasgupta et al., 2005; Johannessen et al., 2005). In contrast to differentiated glia, we observed no change in mTOR pathway activation in CKO mice. Collectively, these results demonstrate that neurofibromin regulates gliogenesis in a Ras-dependent, but mTOR-independent, fashion and suggest that the various downstream Ras effectors have cell type-specific roles in the developing CNS.

Whereas activated Kras or Akt expression in BLBP+ cells recapitulated the glial phenotypes seen in CKO mice, constitutive activation of Kras or Akt did not affect forebrain cortical thickness or neurite length. These findings suggested that neurofibromin might control neuronal differentiation in a Ras-independent manner. Neurofibromin has been previously implicated in cAMP-dependent nervous system development. Loss of neurofibromin in *Drosophila* results in reduced growth and learning deficits that depend on intracellular cAMP levels (Guo et al., 2000; The et al., 1997). In addition, neurofibromin-deficient mouse embryo forebrains exhibit decreased adenylyl cyclase activity and lower cAMP levels (Tong et al., 2002), and cAMP generation by pituitary adenylyl cyclase activating protein (PACAP), a regulator of cortical neuron proliferation and differentiation (Lu and DiCicco-Bloom, 1997; Ohta et al., 2006), is neurofibromin dependent (Dasgupta et al., 2003; Guo et al., 2000).

In support of a cAMP-dependent mechanism underlying neurofibromin regulation of neuronal differentiation, we observed complete rescue of the cortical thickness defect in CKO mice after rolipram treatment in vivo. In addition, increasing cAMP levels in differentiating *Nf1*-deficient neural progenitor cells using either rolipram or forskolin resulted in a partial or near-complete rescue of the CKO neurite length defect in vitro. The cAMP responsive element binding protein (CREB) is one of the major transcription factors driving neuronal differentiation and neuritogenesis as well as cortical development (Chen et al., 2005; Redmond et al., 2002). In CKO mice, we found decreased CREB activation in the brain, reflecting reduced cAMP generation due to neurofibromin loss.

Previous studies have shown that cAMP-dependent signaling is a major regulator of neuronal development and neurite extension in vivo (Fujioka et al., 2004; Nakagawa et al., 2002). Our results strengthen these prior findings by demonstrating a distinct role for neurofibromin cAMP regulation in neuronal differentiation in vitro and in vivo. Additional support for neurofibromin in neuronal development derives from recent studies in which neurofibromin was required for protein kinase A (PKA)-regulated dendritic spine formation in cultured hippocampal neurons in response to syndecan-2 (Lin et al., 2007). These observations coupled with previous studies demonstrating a physical interaction between syndecan-2 and neurofibromin (Hsueh et al., 2001) suggest that neurofibromin cAMP regulation is an important determinant in neuronal differentiation.

Recent findings in *Nf1*-deficient *Drosophila* mutants have argued against separable Ras- and cAMP-related functions (Walker et al., 2006). The findings presented in this report support the idea that there exist distinct Ras- and cAMP-dependent functions for neurofibromin in the developing mammalian brain. Although there may be minor crosstalk between the cAMP-dependent pathway and the Ras pathway, increasing cAMP levels only corrected the CKO neuronal defects and Ras/Akt activation only phenocopied the glial abnormalities seen in CKO mice. Based on these findings, we favor a model of neurofibromin-dependent brain development in which Ras activity is largely responsible for driving gliogenesis while neurofibromin regulation of intracellular cAMP levels is critical for neuronal maturation and neurite extension. This model system provides unique opportunities to study the molecular determinants that underlie neuroglial progenitor cell fate decisions essential for proper brain development and function.

EXPERIMENTAL PROCEDURES

Generation of Transgenic Mice

A 1604 bp 5′ genomic fragment of the mouse BLBP promoter was generated by PCR, inserted upstream of a nuclear targeted Cre and IRES-lacZ fragment, and sequenced in its entirety prior to pronuclear injection into C57BL/6 × CBA mice by the Washington University Mouse Genetics Core. Transgenic mice were identified by genotyping PCR (Bajenaru et al., 2002) and successfully backcrossed with C57BL/6 mice for at least four generations.

Mice

BLBP-Cre transgenic mice were crossed with $Nf1^{flox/flox}$ mice (Zhu et al., 2001) or with Lox-stop-lox(LSL)-$KRas^{G12D}$ mice (Johnson et al., 2001) to generate the BLBP-Cre; $Nf1^{flox/flox}$ (CKO) and BLBP-Cre; LSL-$KRas^{G12D}$ (Kras*) mice, respectively. BLBP-Cre transgenic mice were also crossed with Lox-stop-lox(LSL)-myr-Akt mice (L.E. and E.B.-M., unpublished data) to generate the BLBP-Cre; LSL-myr-Akt (Akt*) mice. BLBP-Cre animals were also mated with R26R-EYFP

mice (Srinivas et al., 2001) to detect Cre-mediated recombination in vivo. All mice were maintained on a C57BL/6 background. BLBP-Cre, LSL-Kras, and LSL-myr-Akt transgenes were used in heterozygous contexts throughout.

X-Gal Staining

Dissected embryos were fixed by 4% paraformaldehyde (PFA) in phosphate buffered (pH = 7.4) saline (PBS) for 1 hr prior to staining with X-Gal (Invitrogen, Carlsbad, CA) as described previously (Bajenaru et al., 2002).

Tissue Preparation

Timed-pregnant mothers were injected intraperitoneally with 50 mg/kg bodyweight bromodeoxyuridine (BrdU, Sigma-Aldrich, St. Louis, MO) 1 hr prior to dissection. Embryo heads were fixed overnight in 4% PFA at 4°C and then transferred into 30% sucrose for 36 hr before embedding into OCT medium for snap-freezing. Brains of PN1 pups were removed for overnight fixation in 4% PFA or snap-frozen. PN8 and PN18 mice were intraperitoneally injected with BrdU 1 or 3 hr prior to perfusion, respectively. Mice were perfused transcardially with PBS and 4% PFA in PBS. After overnight postfixation at 4°C, coronal slices were transferred to 70% ethanol solution prior to paraffin embedding and sectioning.

Immunostaining

Sixteen micron cryostat sections were permeabilized with 0.1% Triton X-100 in PBS prior to blocking and application of primary antibody. For BrdU labeling on frozen sections, DNA was denatured by 2 M HCl for 30 min followed by two rinses of 0.1 M boric acid (pH 8.0) for 5 min at room temperature (RT) before blocking. Five micron paraffin sections were deparaffinized, treated for antigen retrieval, and incubated in 5% serum blocking solution prior to the overnight incubation of primary antibodies at 4°C for 18 hr (Table S1). For BrdU labeling, deparaffinized sections were treated with 0.1% trypsin in PBS for 10 min at room temperature. DNA was denatured by 0.1 M HCl for 10 min at 4°C and 4 M HCl for 30 min at 37°C followed by two rinses of 0.1 M boric acid (pH 8.0) for 5 min at RT prior to blocking. Fluorescent detection was performed with Alexa-labeled secondary antibodies (Molecular Probes, Eugene, OR), whereas horseradish peroxidase-conjugated secondary antibodies (Vector Laboratories) were employed for Vectastain Elite ABC development.

High-power field (20×) regions of interest on three nonconsecutive, plane-matched sections were photographed digitally on a Nikon microscope (Melville, NY). The number of labeled nuclei (APC, BrdU, NeuN, Olig2) or nuclei clearly associated with cytoplasmic filamentous staining (GFAP, NG2) were counted manually with analySIS software (Soft Imaging System Inc, Lakewood, CO). Cell counts were converted to cell density by measuring the area of the high-power field and averaged for each animal.

Golgi Staining

Perfused brains were postfixed in 4% PFA for 48 hr. Two-millimeter coronal sections were transferred into 3% potassium dichromate solution for 5–7 days with daily changes of fresh solution. After a 1 min wash in distilled water, slices were incubated in 2% silver nitrate solution for 3 days. Eighty micron vibrating microtome sections were air dried on glass slides, dehydrated in ethanol and xylene, and mounted.

Embryonic Neural Stem Cell Cultures and In Vitro Differentiation Assay

Neurospheres were established from the telencephalic lobes of E 10.5 $Nf1^{+/+}$, $Nf1^{+/-}$, and $Nf1^{-/-}$ as well as from E 14.5 BLBP-Cre; $Nf1^{flox/flox}$, $Nf1^{flox/flox}$, and BLBP-Cre; LSL-$KRas^{G12D}$ embryos as previously reported (Dasgupta and Gutmann, 2005). Secondary neurospheres were trypsinized, and single-cell suspensions (30,000 cells per ml) were plated on fibronectin-coated cell culture dishes in growth media without EGF and FGF. After 24 hr, cultures were treated with rolipram (20 μM) or forskolin (20 μM). Cells were fixed after 6 days and stained for Tuj1 and BLBP. The longest neurites of at least 30 randomly selected Tuj1+ cells were measured for each experimental condition. The experiments were repeated with independent cultures from at least three embryos.

Western Blot Analysis

Brains were triturated in lysis buffer for 20 min on ice prior to centrifugation at 14,000 rpm for 10 min at 4°C. Equal amounts of total protein as determined using the BCA protein assay kit (Pierce, Rockford, IL) were separated on SDS-PAGE gel. After blocking in 5% dry milk in Tris-buffered saline (TBS), blots were incubated overnight at 4°C with primary antibodies (Table S2) prior to peroxidase-conjugated secondary antibody exposure and detection by Supersignal West Pico enhanced chemiluminescence (Pierce).

cAMP Measurements

Dissected forebrain hemispheres snap-frozen in liquid nitrogen were triturated in ice-cold 5% trichloroacetic acid (10 μl per mg tissue), centrifuged at 1000 × *g* for 10 min at 4°C. Supernatants supplemented with equal volume of 0.1 M HCl were extracted with water-saturated ether thrice prior to desiccation in a vacuum centrifuge. cAMP was determined by using a cyclic AMP enzyme immunoassay kit (Assay Designs, Ann Arbor, MI).

Rolipram Treatment

Rolipram (50 μg in 200 μl PBS with 2% DMSO) was administered to timed-pregnant mothers from 11 days postcoitus (E11.5) until postnatal day 18 (PN18). Pups also received daily i.p. injection of rolipram (12.5 μg) from PN7.

Statistical Analysis

Each experiment was performed with samples from at least three animals from independent litters. Statistical significance ($p < 0.05$) was determined by unpaired t test (with Welch's Correction) using GraphPad Prism 4.0 software (GraphPad Inc., San Diego, CA).

Supplemental Data

Supplemental Data include Supplemental Experimental Procedures, five figures, and two tables and can be found with this article online at http://www.cellstemcell.com/cgi/content/full/1/4/443/DC1/.

ACKNOWLEDGMENTS

We thank Carrie Haipek and Robert Mitchell for technical assistance. We thank Drs. Joshua Rubin and Kevin Ess for their advice and technical suggestions. We thank Dr. Frank Costantini (Columbia University) for the Rosa-YFP, Dr. Tyler Jacks (Massachusetts Institute of Technology) for the LSL-KRAS, and Dr. Luis Parada (University of Texas) for the $Nf1^{flox/flox}$ mice. Dr. Charles Stiles (Dana Farber Cancer Institute) and Dr. Nathaniel Heintz (Rockefeller University) kindly provided the antibodies against Olig2 and BLBP, respectively. This work was supported by grants to D.H.G. (1-UO1-CA84314 and DAMD-17-03-1-0215).

Received: February 3, 2007
Revised: June 28, 2007
Accepted: July 23, 2007
Published: October 10, 2007

REFERENCES

Arnold, D., Feng, L., Kim, J., and Heintz, N. (1994). A strategy for the analysis of gene expression during neural development. Proc. Natl. Acad. Sci. USA *91*, 9970–9974.

Bajenaru, M.L., Zhu, Y., Hedrick, N.M., Donahoe, J., Parada, L.F., and Gutmann, D.H. (2002). Astrocyte-specific inactivation of the neurofibromatosis 1 gene (NF1) is insufficient for astrocytoma formation. Mol. Cell. Biol. *22*, 5100–5113.

Barad, M., Bourtchouladze, R., Winder, D.G., Golan, H., and Kandel, E. (1998). Rolipram, a type IV-specific phosphodiesterase inhibitor, facilitates the establishment of long-lasting long-term potentiation and improves memory. Proc. Natl. Acad. Sci. USA *95*, 15020–15025.

Basu, T.N., Gutmann, D.H., Fletcher, J.A., Glover, T.W., Collins, F.S., and Downward, J. (1992). Aberrant regulation of ras proteins in malignant tumour cells from type 1 neurofibromatosis patients. Nature *356*, 713–715.

Bennett, M.R., Rizvi, T.A., Karyala, S., McKinnon, R.D., and Ratner, N. (2003). Aberrant growth and differentiation of oligodendrocyte progenitors in neurofibromatosis type 1 mutants. J. Neurosci. *23*, 7207–7217.

Benowitz, L.I., and Routtenberg, A. (1997). GAP-43: an intrinsic determinant of neuronal development and plasticity. Trends Neurosci. *20*, 84–91.

Brannan, C.I., Perkins, A.S., Vogel, K.S., Ratner, N., Nordlund, M.L., Reid, S.W., Buchberg, A.M., Jenkins, N.A., Parada, L.F., and Copeland, N.G. (1994). Targeted disruption of the neurofibromatosis type-1 gene leads to developmental abnormalities in heart and various neural crest-derived tissues. Genes Dev. *8*, 1019–1029.

Chen, Y., Wang, P.Y., and Ghosh, A. (2005). Regulation of cortical dendrite development by Rap1 signaling. Mol. Cell. Neurosci. *28*, 215–228.

Dasgupta, B., and Gutmann, D.H. (2005). Neurofibromin regulates neural stem cell proliferation, survival, and astroglial differentiation in vitro and in vivo. J. Neurosci. *25*, 5584–5594.

Dasgupta, B., Dugan, L.L., and Gutmann, D.H. (2003). The neurofibromatosis 1 gene product neurofibromin regulates pituitary adenylate cyclase-activating polypeptide-mediated signaling in astrocytes. J. Neurosci. *23*, 8949–8954.

Dasgupta, B., Yi, Y., Chen, D.Y., Weber, J.D., and Gutmann, D.H. (2005). Proteomic analysis reveals hyperactivation of the mammalian target of rapamycin pathway in neurofibromatosis 1-associated human and mouse brain tumors. Cancer Res. *65*, 2755–2760.

DeClue, J.E., Papageorge, A.G., Fletcher, J.A., Diehl, S.R., Ratner, N., Vass, W.C., and Lowy, D.R. (1992). Abnormal regulation of mammalian p21ras contributes to malignant tumor growth in von Recklinghausen (type 1) neurofibromatosis. Cell *69*, 265–273.

Dromard, C., Bartolami, S., Deleyrolle, L., Takebayashi, H., Ripoll, C., Simonneau, L., Prome, S., Puech, S., Tran Van Ba, C., Duperray, C., et al. (2006). NG2 and olig2 expression provides evidence for phenotypic deregulation of cultured CNS and PNS neural precursor cells. Stem Cells *25*, 340–353.

Fujioka, T., Fujioka, A., and Duman, R.S. (2004). Activation of cAMP signaling facilitates the morphological maturation of newborn neurons in adult hippocampus. J. Neurosci. *24*, 319–328.

Giorgi, M., Modica, A., Pompili, A., Pacitti, C., and Gasbarri, A. (2004). The induction of cyclic nucleotide phosphodiesterase 4 gene (PDE4D) impairs memory in a water maze task. Behav. Brain Res. *154*, 99–106.

Guo, H.F., Tong, J., Hannan, F., Luo, L., and Zhong, Y. (2000). A neurofibromatosis-1-regulated pathway is required for learning in Drosophila. Nature *403*, 895–898.

Hsueh, Y.P., Roberts, A.M., Volta, M., Sheng, M., and Roberts, R.G. (2001). Bipartite interaction between neurofibromatosis type I protein (neurofibromin) and syndecan transmembrane heparan sulfate proteoglycans. J. Neurosci. *21*, 3764–3770.

Hyman, S.L., Shores, A., and North, K.N. (2005). The nature and frequency of cognitive deficits in children with neurofibromatosis type 1. Neurology *65*, 1037–1044.

Jacobson, R.D., Virag, I., and Skene, J.H. (1986). A protein associated with axon growth, GAP-43, is widely distributed and developmentally regulated in rat CNS. J. Neurosci. *6*, 1843–1855.

Johannessen, C.M., Reczek, E.E., James, M.F., Brems, H., Legius, E., and Cichowski, K. (2005). The NF1 tumor suppressor critically regulates TSC2 and mTOR. Proc. Natl. Acad. Sci. USA *102*, 8573–8578.

Johnson, L., Mercer, K., Greenbaum, D., Bronson, R.T., Crowley, D., Tuveson, D.A., and Jacks, T. (2001). Somatic activation of the K-ras oncogene causes early onset lung cancer in mice. Nature *410*, 1111–1116.

Klesse, L.J., and Parada, L.F. (1998). p21 ras and phosphatidylinositol-3 kinase are required for survival of wild-type and NF1 mutant sensory neurons. J. Neurosci. *18*, 10420–10428.

Kurtz, A., Zimmer, A., Schnutgen, F., Bruning, G., Spener, F., and Muller, T. (1994). The expression pattern of a novel gene encoding brain-fatty acid binding protein correlates with neuronal and glial cell development. Development *120*, 2637–2649.

Lakkis, M.M., Golden, J.A., O'Shea, K.S., and Epstein, J.A. (1999). Neurofibromin deficiency in mice causes exencephaly and is a modifier for Splotch neural tube defects. Dev. Biol. *212*, 80–92.

Ligon, K.L., Kesari, S., Kitada, M., Sun, T., Arnett, H.A., Alberta, J.A., Anderson, D.J., Stiles, C.D., and Rowitch, D.H. (2006). Development of NG2 neural progenitor cells requires Olig gene function. Proc. Natl. Acad. Sci. USA *103*, 7853–7858.

Lin, Y.L., Lei, Y.T., Hong, C.J., and Hsueh, Y.P. (2007). Syndecan-2 induces filopodia and dendritic spine formation via the neurofibromin-PKA-Ena/VASP pathway. J. Cell Biol. *177*, 829–841.

Listernick, R., Charrow, J., and Gutmann, D.H. (1999). Intracranial gliomas in neurofibromatosis type 1. Am. J. Med. Genet. *89*, 38–44.

Lu, N., and DiCicco-Bloom, E. (1997). Pituitary adenylate cyclase-activating polypeptide is an autocrine inhibitor of mitosis in cultured cortical precursor cells. Proc. Natl. Acad. Sci. USA *94*, 3357–3362.

Nakagawa, S., Kim, J.E., Lee, R., Malberg, J.E., Chen, J., Steffen, C., Zhang, Y.J., Nestler, E.J., and Duman, R.S. (2002). Regulation of neurogenesis in adult mouse hippocampus by cAMP and the cAMP response element-binding protein. J. Neurosci. *22*, 3673–3682.

Ohta, S., Gregg, C., and Weiss, S. (2006). Pituitary adenylate cyclase-activating polypeptide regulates forebrain neural stem cells and neurogenesis in vitro and in vivo. J. Neurosci. Res. *84*, 1177–1186.

Redmond, L., Kashani, A.H., and Ghosh, A. (2002). Calcium regulation of dendritic growth via CaM kinase IV and CREB-mediated transcription. Neuron *34*, 999–1010.

Romero, M.I., Lin, L., Lush, M.E., Lei, L., Parada, L.F., and Zhu, Y. (2007). Deletion of Nf1 in neurons induces increased axon collateral branching after dorsal root injury. J. Neurosci. *27*, 2124–2134.

Shea, T.B., Dahl, D.C., Nixon, R.A., and Fischer, I. (1997). Triton-soluble phosphovariants of the heavy neurofilament subunit in developing and mature mouse central nervous system. J. Neurosci. Res. *48*, 515–523.

Silva, A.J., Frankland, P.W., Marowitz, Z., Friedman, E., Laszlo, G.S., Cioffi, D., Jacks, T., and Bourtchuladze, R. (1997). A mouse model for the learning and memory deficits associated with neurofibromatosis type I. Nat. Genet. *15*, 281–284.

Singh, S.K., Clarke, I.D., Hide, T., and Dirks, P.B. (2004). Cancer stem cells in nervous system tumors. Oncogene *23*, 7267–7273.

Srinivas, S., Watanabe, T., Lin, C.S., William, C.M., Tanabe, Y., Jessell, T.M., and Costantini, F. (2001). Cre reporter strains produced by targeted insertion of EYFP and ECFP into the ROSA26 locus. BMC Dev. Biol. *1*, 4.

Sundholm-Peters, N.L., Yang, H.K., Goings, G.E., Walker, A.S., and Szele, F.G. (2004). Radial glia-like cells at the base of the lateral ventricles in adult mice. J. Neurocytol. *33*, 153–164.

Taylor, M.D., Poppleton, H., Fuller, C., Su, X., Liu, Y., Jensen, P., Magdaleno, S., Dalton, J., Calabrese, C., Board, J., et al. (2005). Radial glia cells are candidate stem cells of ependymoma. Cancer Cell *8*, 323–335.

The, I., Hannigan, G.E., Cowley, G.S., Reginald, S., Zhong, Y., Gusella, J.F., Hariharan, I.K., and Bernards, A. (1997). Rescue of a Drosophila NF1 mutant phenotype by protein kinase A. Science *276*, 791–794.

Tong, J., Hannan, F., Zhu, Y., Bernards, A., and Zhong, Y. (2002). Neurofibromin regulates G protein-stimulated adenylyl cyclase activity. Nat. Neurosci. *5*, 95–96.

Vogel, K.S., Brannan, C.I., Jenkins, N.A., Copeland, N.G., and Parada, L.F. (1995). Loss of neurofibromin results in neurotrophin-independent survival of embryonic sensory and sympathetic neurons. Cell *82*, 733–742.

Walker, J.A., Tchoudakova, A.V., McKenney, P.T., Brill, S., Wu, D., Cowley, G.S., Hariharan, I.K., and Bernards, A. (2006). Reduced growth of Drosophila neurofibromatosis 1 mutants reflects a non-cell-autonomous requirement for GTPase-Activating Protein activity in larval neurons. Genes Dev. *20*, 3311–3323.

Zhu, Y., Romero, M.I., Ghosh, P., Ye, Z., Charnay, P., Rushing, E.J., Marth, J.D., and Parada, L.F. (2001). Ablation of NF1 function in neurons induces abnormal development of cerebral cortex and reactive gliosis in the brain. Genes Dev. *15*, 859–876.

Zhu, Y., Harada, T., Liu, L., Lush, M.E., Guignard, F., Harada, C., Burns, D.K., Bajenaru, M.L., Gutmann, D.H., and Parada, L.F. (2005). Inactivation of NF1 in CNS causes increased glial progenitor proliferation and optic glioma formation. Development *132*, 5577–5588.